Overproduction of Flotillin Influences Cell Differentiation and Shape in *Bacillus subtilis*

Benjamin Mielich-Süss, Johannes Schneider, Daniel Lopez

Research Center for Infectious Diseases ZINF, Würzburg University, Würzburg, Germany

ABSTRACT Bacteria organize many membrane-related signaling processes in functional microdomains that are structurally and functionally similar to the lipid rafts of eukaryotic cells. An important structural component of these microdomains is the protein flotillin, which seems to act as a chaperone in recruiting other proteins to lipid rafts to facilitate their interaction. In eukaryotic cells, the occurrence of severe diseases is often observed in combination with an overproduction of flotillin, but a functional link between these two phenomena is yet to be demonstrated. In this work, we used the bacterial model *Bacillus subtilis* as a tractable system to study the physiological alterations that occur in cells that overproduce flotillin. We discovered that an excess of flotillin altered specific signal transduction pathways that are associated with the membrane microdomains of bacteria. As a consequence of this, we detected significant defects in cell division and cell differentiation. These physiological alterations were in part caused by an unusual stabilization of the raft-associated protease FtsH. This report opens the possibility of using bacteria as a working model to better understand fundamental questions related to the functionality of lipid rafts.

IMPORTANCE The identification of signaling platforms in the membrane of bacteria that are functionally and structurally equivalent to eukaryotic lipid rafts reveals a level of sophistication in signal transduction and membrane organization unexpected in bacteria. It opens new and promising venues to address intricate questions related to the functionality of lipid rafts by using bacteria as a more tractable system. This is the first report that uses bacteria as a working model to investigate a fundamental question that was previously raised while studying the role of eukaryotic lipid rafts. It also provides evidence of the critical role of these signaling platforms in orchestrating diverse physiological processes in prokaryotic cells.

Bacterial membranes are composed of different types of lipids, which tend to aggregate according to their physicochemical properties and accumulate into lipid domains that are immiscible with the surrounding lipids (1). The heterogeneous organization of membrane lipids leads to a lateral segregation of the embedded membrane proteins, which seems important for their functionality (2). One of the most interesting examples of the heterogeneous segregation of lipids and proteins is the formation of functional microdomains in the membrane of bacteria that are structurally and functionally equivalent to the lipid rafts of eukaryotic cells (3–5). Bacterial microdomains are membrane platforms that organize a group of proteins related to signal transduction and protein secretion (6). The integrity of these signaling platforms is essential for the correct functionality of the harbored proteins. Consequently, any alteration in their architecture severely inhibits the physiological processes related to the harbored proteins, such as biofilm formation, motility, competence, or protease secretion (6, 7).

The integrity of bacterial lipid rafts relies on the biosynthesis and aggregation of polyisoprenoid lipids and the presence of flotillin proteins (6, 8). Flotillins are membrane-bound proteins that localize exclusively in the lipid rafts and are usually considered a bona fide marker for the localization of lipid rafts. The function of flotillins in lipid rafts is not entirely understood, yet it is believed that they may act as chaperone proteins to recruit protein cargo to lipid rafts and facilitate interactions and oligomerization (9–12). Hence, the presence of flotillin in lipid rafts is necessary for the correct functionality of the associated signaling processes. In eukaryotic cells, alterations in the functionality of flotillins often occur in association with severe physiological dysfunctions in cells (13). For instance, the development of Alzheimer's disease or Parkinson's disease is usually observed in cells that concomitantly overproduce flotillin proteins (14, 15), as well as in neuronal cells with severe lesions (16, 17). Despite this interesting correlation, it is still unclear whether the overproduction of flotillin contributes to the physiological alterations or is actually a consequence of the disease. The number of technical challenges associated with the manipulation of eukaryotic cells has complicated the study of the role of flotillins (18). This motivated us to use the bacterium *Bacillus subtilis* as a working model to evaluate whether the overproduction of flotillins causes any alteration in the cellular physiology of the bacterium and whether this effect could possibly result in cellular dysfunction.

The functional membrane microdomains of the bacterial model organism *Bacillus subtilis* contain two structurally similar flotillin-like proteins, which are referred to as FloA (formerly

YqfA) (6, 19) and FloT (formerly YuaG) (6, 8). Cells lacking FloA and FloT are defective in a number of signal transduction pathways that are associated with the protein cargo of the functional membrane microdomains (e.g., biofilm formation, sporulation, motility, or competence) (6, 8, 20, 21). Thus, it is believed that FloA and FloT facilitate the interaction and oligomerization of the protein cargo in the functional microdomains of *B. subtilis* in a fashion similar to that described for eukaryotic lipid rafts. Supporting this hypothesis, a direct interaction of FloA and FloT with the protein cargo protease FtsH (22) has been reported that is important for the protease activity of FtsH. Furthermore, an additional number of FloT-interacting proteins have been identified recently, including a number of proteins related to signal transduction and protein secretion (20). Accordingly, protein secretion was reduced in cells lacking flotillin, which suggests that the associated protein secretion machinery loses its functionality in the absence of flotillin (20).

The first signal transduction pathway described in association with the flotillins of *B. subtilis* leads cells to specialize in the production of extracellular matrix to ultimately form biofilms (6). The induction of this signaling pathway is driven by the activation of the master regulator Spo0A via phosphorylation (Spo0A~P) (23, 24). The membrane-bound sensor kinase KinC, responsible for phosphorylating Spo0A~P, is part of the protein cargo, and its activity depends on the functionality of FloA and FloT (6) in a similar manner to the protease FtsH (22). FtsH is responsible for degrading the phosphatase enzymes that ultimately inactivate Spo0A~P by dephosphorylation (25) and actively contributes to the differentiation of matrix-producing cells (22). Therefore, published data suggest that the signal transduction pathway that is involved in biofilm formation is controlled by regulatory proteins, which localize in the functional membrane microdomains.

Further evidence was presented that exponentially growing *B. subtilis* cells accumulate FloA and FloT in the septum of dividing cells (22), suggesting that flotillins interact with septum-localized proteins, with FtsH as one example of this kind. This suggests a possible involvement of flotillins in processes related to cell division or cell shape. Related to this observation, other laboratories have determined that *B. subtilis* cells lacking flotillins underwent an aberrant cell division process (7). Thus, these two physiological features involving cell division and biofilm formation seemed affected by FloA and FloT in *B. subtilis* cells and could be studied to monitor the functionality of flotillins in *B. subtilis* cells.

In this report, we show that a 5-fold induction in the production of FloA and FloT significantly increased the amount of flotillin harbored in the microdomains, and this severely affected biofilm formation and cell division in *B. subtilis*. The subpopulation of cells specialized to produce extracellular matrix increased due to an implementation of FtsH activity. Cells overproducing FloA and FloT showed a more efficient septation process, which resulted in shortened cells, minicells, and cells with aberrant septa. As a consequence of the FloA and FloT overproduction, an implementation of the FtsH protease activity occurs, which negatively affects the stability of the protein EzrA (Extra Z-rings assembly), an inhibitor of septum formation (26–28). Altogether, overproduction of flotillins severely affected important cellular processes that directly impacted the physiology of the cells and could potentially contribute to the development of severe diseases in other living organisms.

RESULTS AND DISCUSSION

The overproduction of FloT and FloA reached saturation in *B. subtilis*. The bacterial model *B. subtilis* was used to overexpress the *floA* and *floT* genes under the control of an isopropyl-β-D-thiogalactopyranoside (IPTG)-inducible promoter, P_{hp} (the Hyperspank promoter). To first compare the overexpression levels to the natural expression levels, we generated translational fusions of *floA* and *floT* to a green fluorescent protein (GFP) gene (*gfp*) anchored to the cytosolic C-terminal part of the protein. PY79 P_{floA}FloA-GFP-, P_{floT}FloT-GFP-, P_{hp}FloA-GFP-, and P_{hp}FloT-GFP-labeled strains were grown in liquid cultures of the chemically defined medium MSgg at 30°C until they reached the stationary phase (29). Cells were harvested, fixed with paraformaldehyde, and examined with a fluorescence microscope. Expression from the native promoter showed that the fluorescence signal attributable to FloA and FloT was organized as discrete foci across the cellular membrane and was occasionally positioned in the septum of dividing cells, as previously reported (Fig. 1A and B) (22). The strains expressing P_{hp}FloA-GFP and P_{hp}FloT-GFP constructs showed expression levels below the natural level of expression in the absence of IPTG (see Fig. S1 in the supplemental material). Indeed, the addition of IPTG to the cultures induced the expression of FloA and FloT. Fluorescence microscopy analysis showed that 0.1 mM IPTG resulted in expression levels comparable to those of the native promoters (see Fig. S1). Saturation of flotillin levels was achieved by adding 15 mM IPTG to the cell cultures. No significant changes in the expression of FloA or FloT were detected in cells that grew with IPTG concentrations above 15 mM. The presence of IPTG did not cause any significant growth alteration in cultures of the PY79 strain (see Fig. S2 in the supplemental material).

Next, we compared the increment in the relative fluorescence signal between native expression and IPTG-inducible full expression. On average, our results showed that full induction by IPTG caused an approximately 5-fold increase in the production of FloA and FloT fluorescence signals in comparison to the native expression level. Further examination at the single-cell level showed that the induction of FloA and FloT expression resulted in an increase of the fluorescence intensity of the membrane foci and, to a lesser extent, in the number of foci. Figure 1C and D show the analysis of the subcellular organization of the fluorescence signal in representative single cells expressing FloA-GFP and FloT-GFP at native and full induction levels, respectively.

Saturation of FloT and FloA affects biofilm formation and cell differentiation. Biofilm formation in *B. subtilis* requires the differentiation of numerous cell types. Among those, the matrix-producing cell type is responsible for the production and secretion of the extracellular matrix of the biofilm (24, 30, 31). The subpopulation of matrix producers simultaneously expresses the *epsA-O* operon (henceforth called the *eps* operon) and the *tapA-sipW-tasA* operon (henceforth called the *tasA* operon). The *eps* operon encodes the enzymes responsible for the production of the extracellular exopolysaccharide (32–34). The *tasA* operon is required for the production of extracellular amyloid fibers that structurally give consistency to the biofilm (35–39).

To investigate whether the overexpression of FloA and FloT affects biofilm formation, strains overproducing FloA and FloT were constructed and used to assay biofilm formation. The morphology of *B. subtilis* colonies grown on solid biofilm-inducing
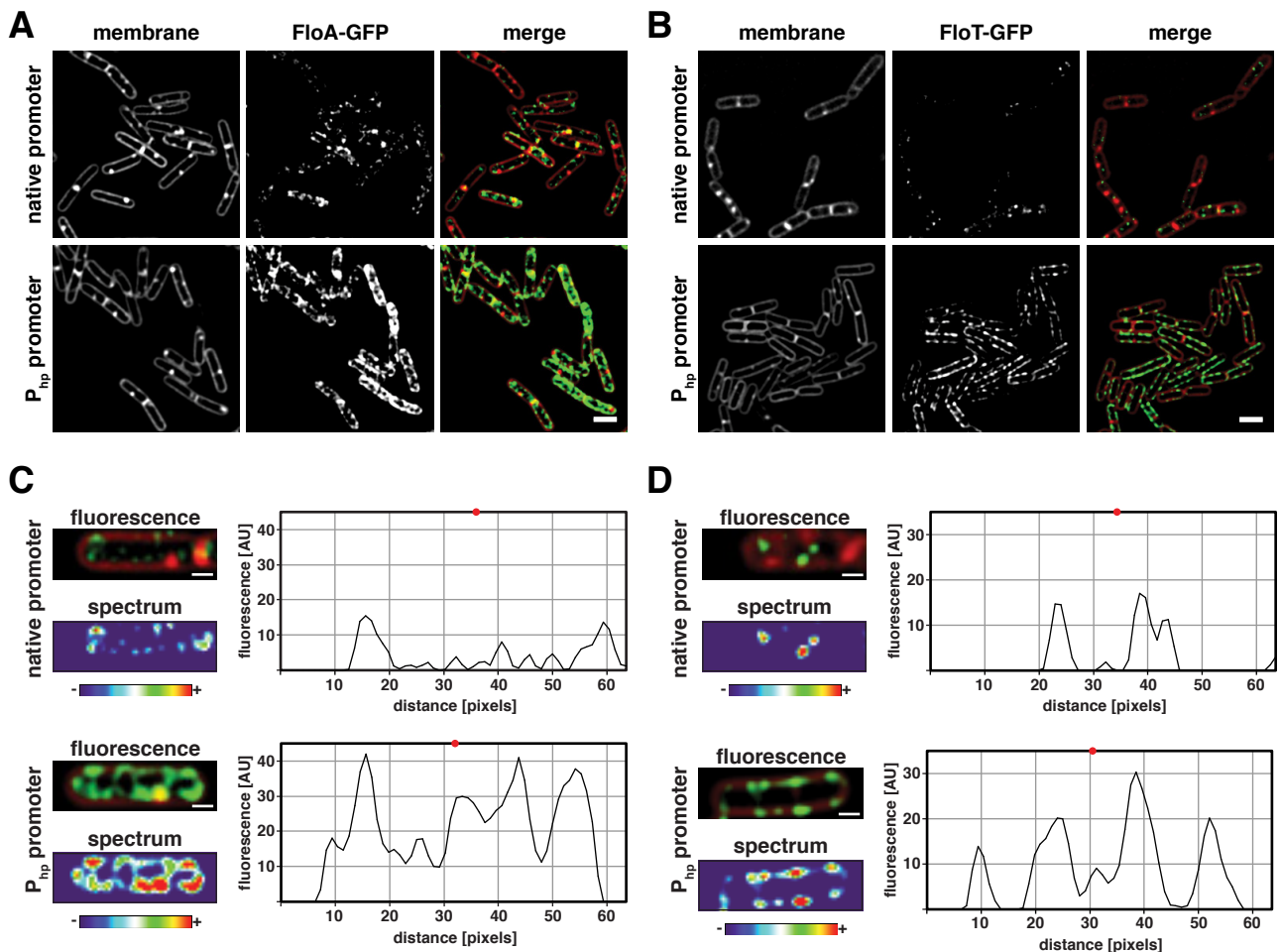
FIG 1 Saturation of FloA and FloT in functional membrane microdomains of *B. subtilis*. Shown are levels of expression in cells expressing FloA-GFP (A) or FloT-GFP (B) under the control of an IPTG-inducible promoter (P_{hp}) (bottom row) compared to natural expression levels obtained with their native promoters (upper row). Cells were grown in MSgg medium until they reached the stationary phase. IPTG was added to a final concentration of 15 mM. Membrane staining (left column) was performed with FM4-64 membrane dye. The center column shows the fluorescence signal emitted by the GFP. The right column shows the merged signals. The FM4-64 signal is false colored in red, and GFP is false colored in green. Scale bars are 2 μm. (C and D) Quantification of the fluorescence signal in single cells expressing FloA-GFP and FloT-GFP. The upper row shows the fluorescence signal obtained when expressed under the control of their native promoters. The bottom row shows the fluorescence signal obtained when expressed under the control of an IPTG-inducible promoter. The fluorescent micrographs show membrane staining false colored in red and the GFP fluorescence signal false colored in green. Additionally, the relative GFP fluorescence signal is quantified in relation to the background fluorescence, using a color spectrum logarithmic scale. (The spectrum scale is presented on the bottom.) The relative fluorescence intensity values of each micrograph are represented in a graph (on the left of each micrograph). The *x* axis represents the cell length (in pixels), and the *y* axis represents the value of relative fluorescence intensity detected (in arbitrary units [AU]). The midcell is marked with a red dot. The scale bar is 1 μm.

MSgg agar medium was examined. To generate biofilms on agar, 3 μl of an LB preculture was spotted on MSgg medium supplemented with 15 mM IPTG and allowed to grow at 30°C for 72 h. After incubation, the biofilms develop into integrated microbial communities with great complexity, manifested by the number of wrinkles present on the surface of the biofilm, which is representative of the robustness and the consistency of the extracellular matrix of the biofilm. Two different genetic backgrounds were used to perform this assay—the PY79 and NCIB3610 strains. Strain PY79 is a laboratory strain that is partially deficient in biofilm formation due the acquisition of a point mutation in the *eps* operon (Fig. 2A) (40). While this strain still possesses an intact *tasA* operon, the lack of extracellular polysaccharide makes the PY79 microbial communities flat, and they lack any distinctive complex architecture (40). A deletion of the transcriptional re-

pressor SinR, which uncouples the regulation of the biofilm (33, 41), resulted in a slightly wrinkled colony even in the absence of a functional *eps* operon, suggesting that overexpression of the TasA strain partially restored biofilm formation when overproduced in the PY79 strain. Accordingly, the double mutant $\Delta sinR$ $\Delta tasA$ strain showed a biofilm-null phenotype, suggesting that biofilms generated by PY79 are mainly caused by expression of TasA (Fig. 2B). In contrast, the NCIB3610 strain (henceforth 3610) is the undomesticated *B. subtilis* strain and is considered the ancestor strain of PY79 (32). This strain possesses intact and functional *eps* and *tasA* operons and shows a great ability to form biofilms. Mutations in the *eps* or the *tasA* operons significantly reduce the ability of this strain to form biofilm, and a depletion of SinR results in a hyperwrinkled colony that overproduces extracellular matrix (see Fig. S3 in the supplemental material).
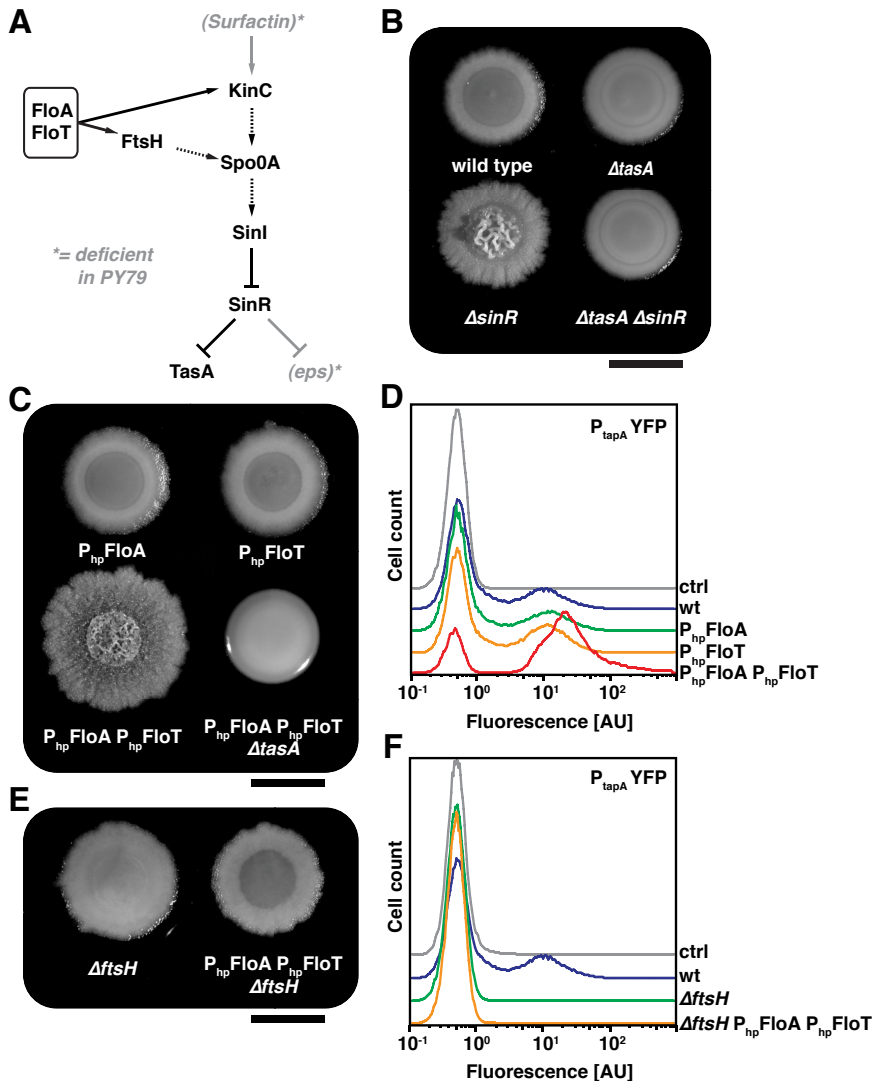
FIG 2 Overexpression of the flotillin-like proteins FloA and FloT promotes biofilm formation via FtsH. (A) Schematic representation of how FloA and FloT influence the signaling pathway leading to matrix production. Spo0A is activated by phosphorylation (Spo0A~P) and indirectly derepresses the expression of the *eps* and *tapA* operons. Phosphorylation of Spo0A~P is driven by the action of the membrane-bound kinase KinC, which is stabilized by FloA and FloT. Spo0A~P is subjected to dephosphorylation by a pool of phosphates that are degraded by the protease FtsH. The activity of FtsH is dependent on FloA and FloT. Solid arrows denote direct regulation, and dashed arrows denote indirect regulation. The asterisk denotes mutations in PY79. (B) Colonies of diverse mutants in the PY79 strain grown in MSgg agar medium for 72 h at 30°C. (C) Effects of flotillin overexpression in colony morphology of PY79 grown on solid MSgg agar medium for 72 h at 30°C with 15 mM IPTG. The scale bar represents 0.5 cm. (D) Flow cytometry analysis to monitor the subpopulation of matrix-producing cells in different genetic backgrounds using the P*tapA*-*yfp* reporter system. Cells were grown for 72 h on solid MSgg medium in the presence of 15 mM IPTG. Approximately 50,000 ungated cells were analyzed. Fluorescence is represented in arbitrary units (AU). ctrl, control; wt, wild type. (E) Diverse mutants in the PY79 genetic background grown on MSgg medium and incubated for 72 h at 30°C supplemented with 15 mM IPTG. The scale bar represents 0.5 cm. (F) Flow cytometry analysis to monitor the subpopulation of matrix-producing cells in different genetic backgrounds that lack FtsH using the P*tapA*-*yfp* reporter system. Cells were grown for 72 h on solid MSgg medium in the presence of 15 mM IPTG. Approximately 50,000 ungated cells were analyzed.

Strains expressing P$_{hp}$FloA, P$_{hp}$FloT, and P$_{hp}$FloA P$_{hp}$FloT were constructed in different genetic backgrounds. The resultant strains were assayed for variations in their ability to form biofilm by allowing them to grow in agar MSgg medium supplemented with 15 mM IPTG at 30°C for 72 h. After incubation, the biofilms

of the strains overexpressing FloA or FloT were morphologically indistinguishable from the wild-type strain, indicating that the overexpression of a single flotillin protein did not influence biofilm formation (Fig. 2C). However, the P$_{hp}$FloA P$_{hp}$-FloT strain that simultaneously overexpressed FloA and FloT resulted in a more robust, biofilm-like colony morphology that was especially evident in the experiments that used the PY79 strain (Fig. 2C; see Fig. S3 in the supplemental material to compare it to other genetic backgrounds). Because PY79 harbors a nonfunctional *eps* operon, we reasoned that the biofilm formation phenotype observed in the PY79 P$_{hp}$FloA P$_{hp}$FloT strain was attributable to the overexpression of TasA protein and the high production of amyloid fibers. A similar effect was observed in the experiments that used the 3610 strain, although this genetic background showed milder effects for reasons that are unknown to us. Hence, based on the robustness and the consistency of the biofilm formation phenotype observed in the PY79 strain, we used this genetic background to further explore the molecular effects in cell differentiation associated with the overproduction of FloA and FloT in *B. subtilis*.

Subsequently, we tested whether the overexpression of *tasA* was responsible for the acquisition of biofilm formation in the PY79 P$_{hp}$FloA P$_{hp}$FloT strain. To do this, we first compared the subpopulation of *tasA*-expressing cells in the wild-type strain and the flotillin-overexpressing strains. All strains were labeled with the yellow fluorescent protein (YFP) transcriptional fusion P*tapA*-*yfp* and grown in MSgg medium plus IPTG (15 mM) at 30°C for 72 h. After incubation, cells were harvested and fixed with 4% paraformaldehyde. The fluorescence signal of 50,000 cells was monitored by flow cytometry and plotted on the graph presented in Fig. 2D. An unlabeled strain served as negative control with the absence of fluorescence signal. The wild-type strain harboring the P*tapA*-*yfp* reporter served as a positive control, where the subpopulation of matrix producers represented approximately 30% of the total cell count. Overproduction of FloA or FloT did not alter the size of this subpopulation. However, when we assayed the size of the subpopulation of matrix producers in the P$_{hp}$FloA P$_{hp}$FloT strain, we detected a 3-fold increase in the number of cells that highly expressed the P*tapA*-*yfp* reporter, suggesting that the overproduction of FloA and FloT led the cells to excessively produce

TasA, which ultimately induced biofilm formation in the PY79 strain.

Overproduction of flotillin stimulates FtsH activity. The genetic cascade responsible for the differentiation of matrix producers is triggered by phosphorylation of Spo0A~P. The membrane kinase KinC induces Spo0A~P phosphorylation in response to the secretion of the signal surfactin (Fig. 2A) (42). Moreover, the activity of the membrane-bound protease FtsH is equally important for matrix production, because FtsH degrades the phosphatases that are responsible for the deactivation of Spo0A~P by dephosphorylation (25). Importantly, both KinC and FtsH proteins localize to the functional membrane microdomains in *B. subtilis*, and their functionality is dependent on the activity of FloA and FloT (6, 22). Figure 2A shows an overview of the regulatory cascade leading to biofilm formation.

We hypothesized that the molecular mechanism underlying the evident increase in the subpopulation of matrix producers could be related to the positive effects of FloA and FloT on the activity of KinC or FtsH. Importantly, the PY79 strain is not able to produce surfactin due to the acquisition of a point mutation in the *sfp* gene during laboratory domestication (Fig. 2A) (40). The Sfp protein is a phosphopantetheinyl transferase that posttranslationally modifies the surfactin biosynthesis machinery. This is an essential process for the correct functionality of the surfactin biosynthesis machinery (43, 44). Thus, the activation of KinC via surfactin is not possible in the PY79 strain. This fact led us to focus on the activity of the membrane-bound protease FtsH.

FtsH indirectly affects the levels of Spo0A~P by degrading four regulatory phosphatase proteins, RapA, RapB, RapE, and Spo0E, which feed into the Spo0A phosphorelay to ultimately decrease the levels of Spo0A~P. The absence of FloA and FloT negatively affects the FtsH protein (22), which prevents the degradation of the RapA, RapB, RapE, and Spo0E phosphatases (25). To explore whether the overproduction of FloA and FloT decreased the levels of Spo0A~P via FtsH, we deleted the *ftsH* gene in the wild-type and P_{hp}FloA P_{hp}FloT strains, and we monitored biofilm formation. The $\Delta ftsH$ and $\Delta ftsH$ P_{hp}FloA P_{hp}FloT strains were grown in MSgg agar medium supplemented with 15 mM IPTG and were incubated at 30°C for 72 h. After incubation, the microbial communities of the $\Delta ftsH$ P_{hp}FloA P_{hp}FloT strain showed no particular biofilm architecture but a flat morphology comparable to that of the wild-type and $\Delta ftsH$ strains (Fig. 2E). Next, these strains were labeled with the P_{tapA}-*yfp* transcriptional fusion to monitor possible variations in the subpopulation of matrix producers by using flow cytometry. Flow cytometry analysis showed that the overproduction of FloA and FloT did not differentiate the subpopulation of matrix producers in cells lacking FtsH (Fig. 2F). This suggests that FtsH mediated the differentiation of matrix producers when FloA and FloT were artificially overproduced.

These results are in agreement with published literature showing that the oligomerization of FtsH in *E. coli* requires the chaperone activity of HflC and HflK, two proteins that are structurally similar to FloA and FloT (45–48). *B. subtilis* lacks the HflC and HflK proteins, and thus, it is possible that FloA and FloT might play the role of HflC and HflK in stabilizing FtsH in *B. subtilis*. To test this hypothesis, whole-cell extracts of the P_{hp}FloA P_{hp}FloT strain were used to semiquantitatively detect FtsH by immunoblot analysis using polyclonal antibodies against FtsH. An increase in FtsH protein was detected in normalized cell extracts from the P_{hp}FloA P_{hp}FloT strain compared to the wild-type strain

(Fig. 3A). Next, we observed that these higher levels of FtsH coincided with higher levels of TasA. We performed an immunoblot analysis using polyclonal antibodies against TasA. The extracts of cells that overproduced FloA and FloT, which showed higher levels of FtsH, also showed higher levels of TasA. Importantly, when the *ftsH* gene was deleted, the detection of TasA was not possible in the strain that overproduced FloA and FloT (Fig. 3B).

Altogether, the data are consistent with the hypothesis that the functional link between FloA/FloT and FtsH mediated the increase of the subpopulation of matrix-producing cells in the PY79 strain that overproduced FloA and FloT. This, in turn, caused an increase in the production of TasA, which resulted in an overproduction of biofilm formation. In those lines, the interaction of FtsH-like proteins with flotillin-like proteins has been described in many systems and organelles (e.g., mitochondria, yeast, or plants), and it has been shown that the stability of FtsH-like proteins depends on the presence of flotillin-like proteins (49, 50). It is hypothesized that the chaperone activity of the flotillin-like proteins acts as a regulator to fine-tune the proteolytic activity of FtsH (49, 50). It also is suggested that flotillins serve as scaffolding proteins to limit the mobility of the FtsH protease across the membrane (49). Based on these current hypotheses, it is probably not surprising that the overproduction of FloA and FloT affected the activity of FtsH of *B. subtilis*.

Flotillin overexpression results in decreased cell length. FtsH principally localizes to the septum of dividing cells (51), where the interaction with FloA and FloT presumably occurs (22). Possibly, flotillins provide stability to protein septum-associated proteins. Accordingly, there is evidence of a significant number of septum-localized proteins among the interactome of FloT (20, 22). Furthermore, the absence of flotillins in *B. subtilis* has been associated with pleiotropic effects on cell shape (7), which led us to reason that septum-localized membrane microdomains could influence septum-associated processes, like septum formation or shape determination.

Septum formation and cell shape determination were analyzed at the single-cell level in cells that overproduced flotillins. To do this, the P_{hp}FloA, P_{hp}FloT, and P_{hp}FloA P_{hp}FloT strains were grown in liquid MSgg medium plus IPTG (15 mM) at 37°C with vigorous agitation until the late exponential growth phase (optical density at 600 nm [OD_{600}] of 0.8 to 1.0). After incubation, cells were stained with the membrane dye FM4-64 before examination under the fluorescence microscope. We observed that under these growth conditions, the simultaneous overexpression of FloA and FloT resulted in a dramatic reduction of cell length (Fig. 4A, column 4; see Fig. S4 in the supplemental material). We randomly selected 500 cells from each microscopic field and measured the cell length (Fig. 4B). On average, wild-type cells showed a cell length of 2.41 ± 0.52 μm. This result was comparable to the length of cells expressing FloA (2.47 ± 0.60 μm) or FloT (2.34 ± 0.65 μm). However, overproduction of FloA and FloT resulted in a cell length of 1.11 ± 0.52 μm. Probably as a consequence of the reduction of cell length, P_{hp}FloA P_{hp}FloT cells also showed a partial loss of the typical *B. subtilis* rod shape, and a subfraction of cells (approximately 19% of the total) became spherical. Among those, we detected a significant number of small, circular, anucleate minicells (approximately 28% of the total) (52–54), as well as small, spherical cells that contained DNA (72% of the total).

The effect on cell length associated by the overexpression of FloA and FloT pointed to an influence of flotillins on the efficiency
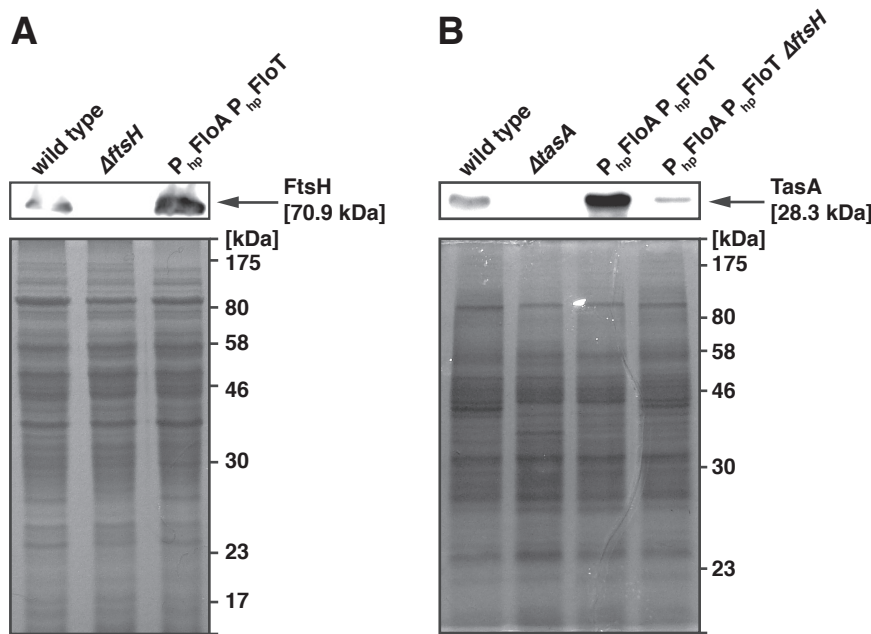
FIG 3 Overproduction of FloA and FloT increase the levels of FtsH and TasA proteins. (A) Immunoblot analysis to detect FtsH in different mutants using polyclonal antibodies against FtsH. The wild-type strain is used as a positive control, while the Δ*ftsH* mutant is used as a negative control. The immunoblot signal is presented in the upper panel, and the respective SDS-PAGE result is presented in the lower panel as a loading control. (B) Detection of TasA production in different mutants by immunoblot analysis using polyclonal antibodies against TasA. The wild-type strain (PY79) is used as a positive control, while the Δ*tasA* mutant is used as a negative control. The immunoblot signal is presented in the upper panel, and the respective SDS-PAGE result is presented in the lower panel. Samples were obtained from the extracellular protein fraction of pellicles that were grown in liquid cultures for 24 h at 30°C. Protein levels were normalized relative to cell number.

of septum formation. To investigate the influence of FloA and FloT in the assembly of proteins with a relevant role in septum formation, we chose the FtsZ protein as a septum-related protein to monitor septum formation in *B. subtilis* cells. FtsZ forms a ring structure (Z-ring) to ultimately drive cell septation (55, 56), and mutants showing an increase in FtsZ assembly also showed additional division events per cell cycle, with the formation of extra septa that led to the occurrence of a minicell-like phenotype (55, 57). Thus, the phenotypic similarities between cells overexpressing FloA and FloT and cells with increases in FtsZ assembly led us to hypothesize a functional connection between these two genotypes. We first tested whether the overproduction of FloA and FloT affects the septation efficiency. To do this, cultures of the P_{hp}FloA P_{hp}FloT mutant were grown in liquid MSgg medium with vigorous agitation, and the cell length was measured at early stages of exponential growth (OD_{600} of 0.1). Our measurements of cell length showed that actively dividing cells were substantially shorter when overproducing FloA and FloT than wild-type cells (Fig. 5A). To elucidate if the reduction of cell length involved FtsZ, we constructed the P_{xyl}FtsZ-GFP and P_{hp}FloA P_{hp}FloT P_{xyl}FtsZ-GFP strains that expressed a labeled FtsZ under the control of a xylose-inducible promoter. In these strains, transcription of FtsZ-GFP is strictly dependent on the amount of xylose that was added to the cultures. This allowed us to correlate the variations in the FtsZ-GFP protein levels to the differences in protein processing or stability. We used these strains to determine that cell length per FtsZ ring (L/R ratio) (58) was significantly reduced in cells overexpressing FloA and FloT in comparison to that in the wild-type strain (Fig. 5B and C). Furthermore, cultures of cells that overproduced FloA and FloT showed a significant increase in the number

of Z-rings compared to that in the wild-type strain (Fig. 4D), suggesting an increase in the number of Z-rings in the shorter cells that overproduced FloA and FloT.

We revisited the pool of proteins associated with the functional membrane microdomains in *B. subtilis* to find those proteins whose activity affects the assembly of the Z-ring. To purify the protein fraction associated with the functional membrane microdomains, the membrane fraction was treated with nonionic detergents and separated by centrifugation in a sucrose gradient. This resulted in one fraction that was sensitive to detergents and another fraction that is composed of larger membrane fragments that were more resistant to detergent disruption (detergent-resistant membrane [DRM] fraction). It is known that the DRM fraction is enriched in proteins associated with lipid rafts (4, 59, 60) and is the fraction that contains the proteins of the functional membrane microdomains when assayed with *B. subtilis* membranes. We detected the protein EzrA in the DRM fraction of *B. subtilis*, with identification coverage of 53% (see Fig. S5 in the supplemental material) (22). EzrA is a negative regulator of the assembly of the Z-ring that localizes in the midcell in an FtsZ-dependent manner. Cells depleted of EzrA (Extra Z-rings assembly) show multiple Z-rings located at the polar and medial sites (27, 61). We hypothesized that overproduction of FloA and FloT could negatively affect the activity of EzrA to promote an accelerated assembly of FtsZ.

To address this question, we generated P_{xyl}EzrA-GFP and P_{hp}FloA P_{hp}FloT P_{xyl}EzrA-GFP strains to compare the levels of expression of EzrA in cells overexpressing FloA and FloT. Examination of cells under the fluorescence microscope did not render conclusive results. Instead, we performed a semiquantitative im-
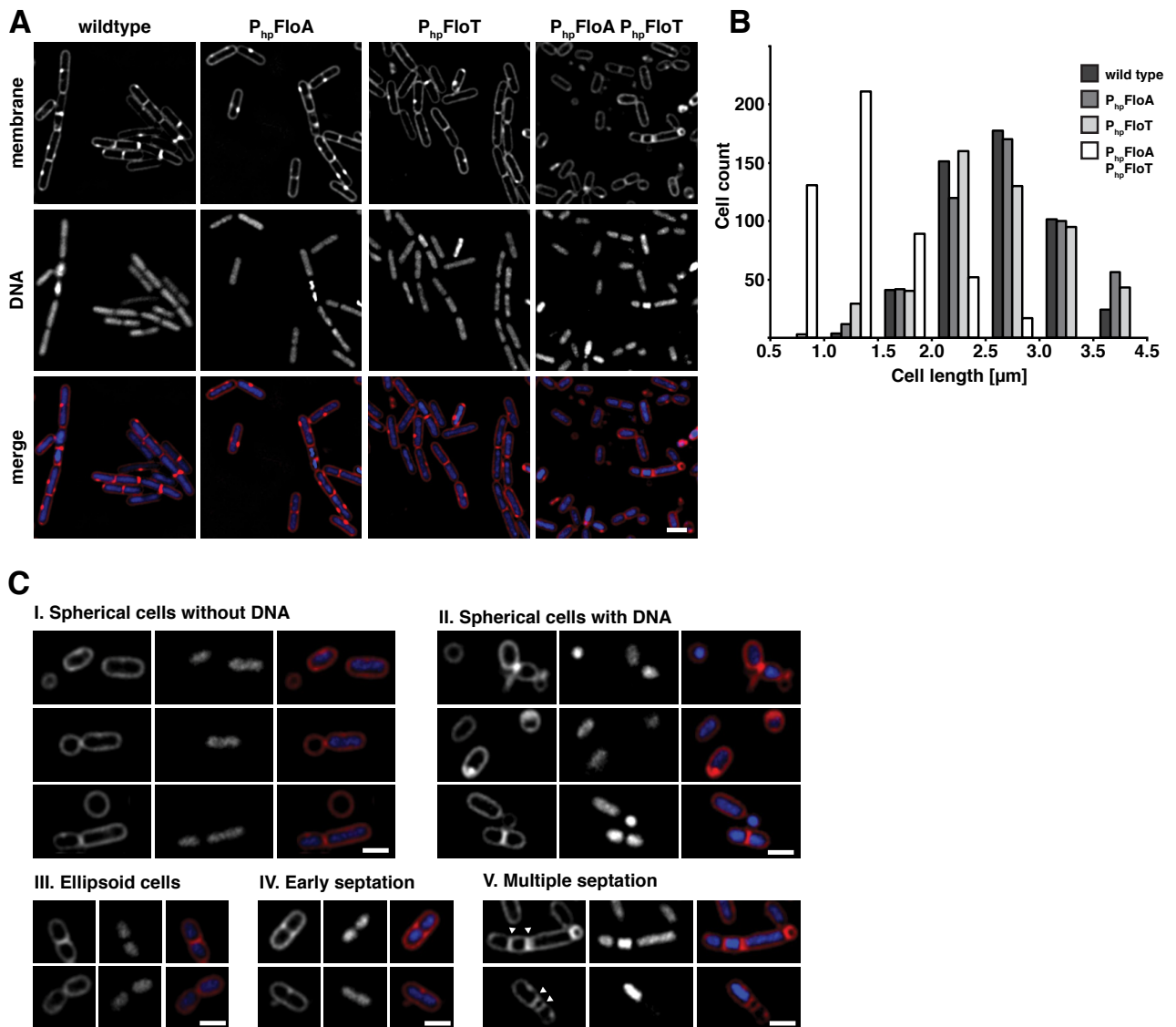
FIG 4 Overexpression of FloA and FloT affects cell shape. (A) Fluorescence micrographs of strains overexpressing FloA, FloT, or both FloA and FloT compared to wild-type cells. The upper row presents membrane staining using FM4-64. The center row shows DNA staining using Hoechst 33342. The bottom row shows the merge of the previous images, with the membrane staining false colored in red and the DNA staining false colored in blue. Cells were grown in liquid MSgg medium at 37°C until they reached the late exponential growth phase. IPTG was added to a final concentration of 15 mM. The scale bar represents 2 μm. (B) Histogram representing the variation in cell length in the different mutants. The number of the cells considered for this analysis was 500. The cell count is represented in the *y* axis. Calculation of cell length was performed using Leica Application Suite Advance Fluorescence software. (C) Detailed view of cell shape aberrations in cells that simultaneously overexpressed FloA and FloT. Spherical cells are shown in panel I. Spherical anucleate cells are shown in panel II. Elipsoid cells are shown in panel III, and cells with a failure in septation are shown in panels IV and V. The scale bars represent 2 μm.

munoblot assay using polyclonal antibodies against GFP. Using this assay, we observed a significant reduction of EzrA levels in the extracts of the P_{hp}FloA P_{hp}FloT P_{xyl}EzrA-GFP strains in comparison to the P_{xyl}EzrA-GFP strain (Fig. 6A). Although this result explained the higher efficiency to form Z-rings and septates in cells overproducing FloA and FloT, it was somewhat unexpected, as one might anticipate that an enhanced chaperone activity of flotillins should always affect the stability of the associated proteins in a positive fashion. One plausible hypothesis that could explain this result is that additional proteins that are stabilized by FloA and FloT negatively influence EzrA. Supporting this hypothesis, we found evidence in the literature that EzrA of *B. subtilis* is

degraded by an ATP-dependent protease that is structurally similar to FtsH (62), suggesting that FtsH could target EzrA in the strain that overexpressed FloA and FloT. This is consistent with the filamentous growth that is described in the mutant lacking FtsH, which is also observed in strains with defective cell septation (63). Consequently, we tested whether FtsH influenced the reduced levels of EzrA observed in cells overexpressing FloA and FloT. To do this, the levels of EzrA-GFP were tested in the presence or absence of FtsH by semiquantitative immunoblot assays, using whole-cell extracts of the P_{hp}FloA P_{hp}FloT P_{xyl}EzrA-GFP and Δ*ftsH* P_{hp}FloA P_{hp}FloT P_{xyl}EzrA-GFP strains. Using this approach, we observed that cells lacking FtsH showed increased lev-
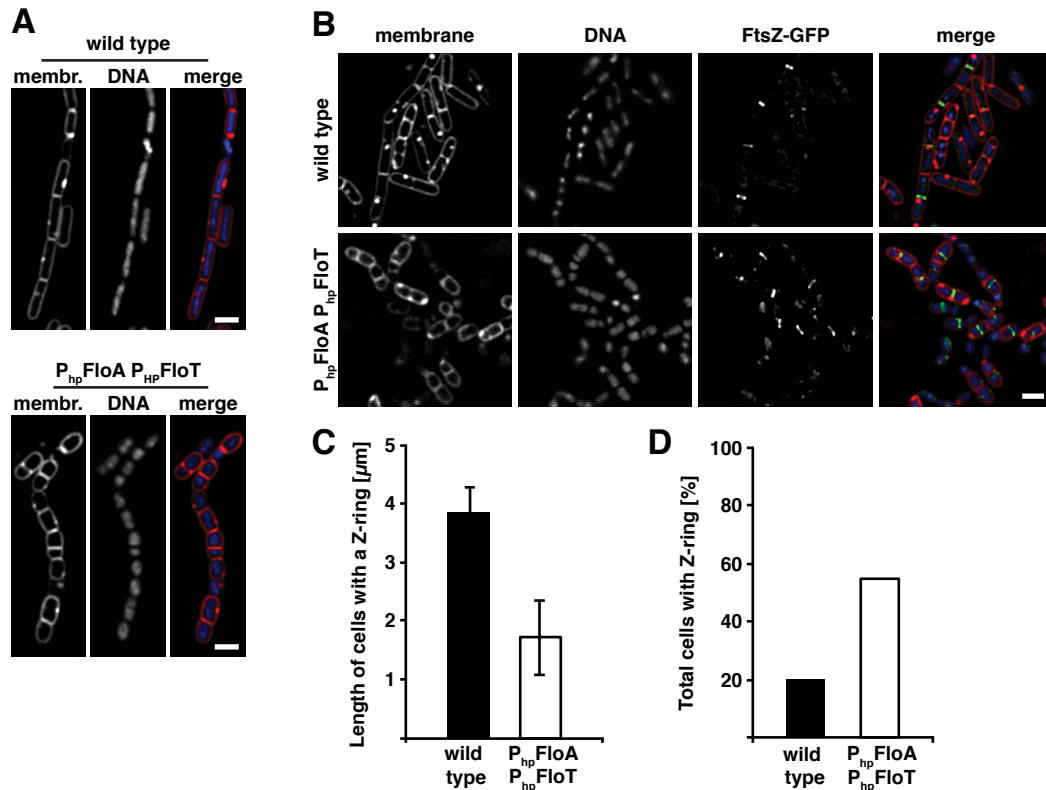
FIG 5 Simultaneous overproduction of FloA and FloT affects formation of the division septum and formation of the Z-ring. (A) Comparison between wild-type cells and the $P_{hp}FloA$ $P_{hp}FloT$ strain during the early exponential growth phase. Cells were grown in liquid MSgg medium at 37°C until they reached an OD_{600} of 0.1. For overexpression, the medium was supplemented with 15 mM IPTG. The membrane (membr.) was stained with FM4-64 (left panel), and the DNA was visualized with Hoechst 33342 (middle panel). The right panel shows merges of the two signals, with the membrane false colored in red and DNA false colored in blue. The scale bar represents 2 μm. (B) Visualization of Z-ring formation in a wild-type strain and the $P_{hp}FloA$ $P_{hp}FloT$ strain bearing an FtsZ-GFP fusion. The first column shows the membrane stained with FM4-64, the second column shows the DNA stained with Hoechst 33342, and the third column shows the FtsZ-GFP signal. In the fourth column, all signals were merged, with the membrane false colored in red, the DNA false colored in blue, and the GFP false colored with green. The cells were grown in liquid MSgg medium at 37°C and harvested in the exponential growth phase. IPTG was added to the growth medium at a final concentration of 15 mM, and basal induction of FtsZ-GFP was achieved with 1% (wt/vol) xylose. The scale bar is 2 μm. (C) Graphical illustration of the length of cells with a visible Z-ring. Approximately 500 cells were used for counting. (D) Graphical illustration of the percentage of cells with a Z-ring; approximately 500 cells were used for counting.

els of EzrA (Fig. 6B). Moreover, we generated the $P_{hp}FtsH$ $P_{xyl}EzrA$-GFP strain, which overexpressed $P_{hp}FtsH$, and whole-cell extracts of this strain were used to compare the abundance of EzrA before and after FtsH overproduction. Figure 6B shows that the overproduction of FtsH was associated with reduced EzrA levels. We detected an intriguing protein band in this strain that could be attributed to an alternative processed form of EzrA protein. More experiments should be performed in this direction to fully address whether a direct interaction exists between FtsH and EzrA. Experiments presented in this report are consistent with the idea that the overexpression of flotillins causes severe physiological changes in bacterial cells.

Overall, our study showed that overexpression of FloA and FloT in the functional membrane microdomains of *B. subtilis* resulted in severe defects in cell differentiation and cell shape. We provide evidence that physiological alterations were mediated by an unusual activity of the FtsH protease (22). We expect that other yet unknown molecular mechanisms may participate in this phenotype, since numerous signal transduction pathways are harbored in the functional membrane microdomains of *B. subtilis*.

Among those, we consider particularly interesting the dual role of the FtsH protease in regulating bacterial cell differentiation and cell shape, as illustrated in Fig. 7. It is probably not surprising that this important regulatory node localizes in the functional membrane microdomains, under the direct control of the two flotillin-like proteins FloA and FloT, in a manner similar to that found in other biological systems (49, 50). Yet, when focusing on *B. subtilis*, it is still unknown whether both FloA and FloT play redundant functions in the functional microdomains. Further experiments are necessary to clarify why the overexpression of two structurally different flotillin proteins is required to achieve the described effects. We tend to think that FloA and FloT are partially redundant and some physiological processes are functionally linked to both FloA and FloT, while other physiological processes are specifically linked to FloA or FloT.

MATERIALS AND METHODS

Strains, media, and culture conditions. For general purposes, the *B. subtilis* strains PY79 and NCIB3610 were used in this study. *Escherichia coli* DH5α was used for cloning purposes. A detailed list of the genetically
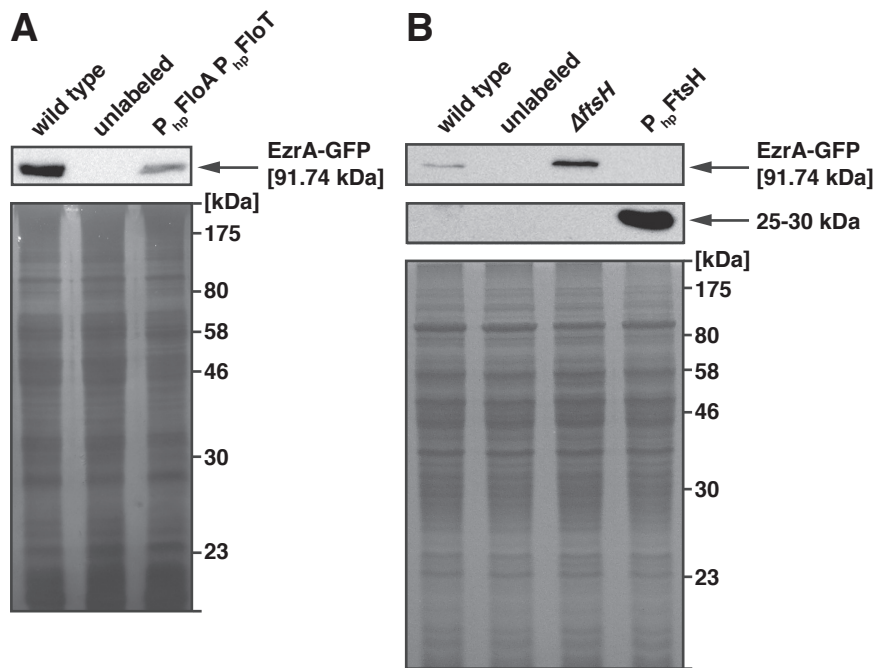
FIG 6 Levels of EzrA are influenced by FtsH. (A and B) Western blot analysis of whole-cell extracts of different mutants to detect the level of EzrA-GFP using polyclonal antibodies against GFP. The extra protein band is shown at 25 to 30 kDa in panel B, which was only detected in the extract of cells that overproduced FtsH. SDS-PAGE results are shown as loading controls. The protein amount was normalized relative to cell number.

modified strains is shown in Table S1 in the supplemental material. For routine growth, cells were propagated on LB medium. Selective media were prepared in LB agar using the antibiotics (final concentrations in parentheses) ampicillin (100 μg/ml), kanamycin (50 μg/ml), chloramphenicol (5 μg/ml), tetracycline (5 μg/ml), spectinomycin (100 μg/ml), and erythromycin (2 μg/ml) plus lincomycin (25 μg/ml) for macrolide-lincosamide-streptogramin B (MLS) determination. Biofilm assays and growth of cells for microscopy or biochemical analysis were performed with MSgg medium (29). When required, MSgg culture medium was supplemented with 1% threonine. Unless otherwise stated, induced expression was achieved with 1 mM IPTG or 1% (wt/vol) xylose. To generate biofilms, 3 μl of an LB overnight culture was spotted onto 1.5% agar MSgg plates and incubated for 72 h at 30°C. For liquid cultures, an overnight culture was diluted 1:20 in MSgg medium and grown at 30°C with agitation at 200 rpm until reaching the desired growth stage. If necessary, inducers were added to the culture as stated in the figure legends.

Strain construction. Genomic modifications in *B. subtilis* were performed according to standard protocols (64). Linearized plasmid DNA or PCR products were brought into cells by inducing natural competence, leading to incorporation of the foreign DNA into the genome by heterologous recombination (65). SPP1-mediated phage transduction was used to shuttle constructs among strains, in order to combine mutant alleles (66). For plasmid construction, genes were amplified from genomic DNA with primers carrying a 5′ extension with desired restriction sites to clone the PCR product into the target plasmids. A list of all of the primers used in this study is presented in Table S2 in the supplemental material. For overexpression with the IPTG-inducible Hyperspank promoter, the genes were cloned into pDR111 (67, 68) or into the pBM001 plasmid, a chimera of pDR111 and pDR183 (kindly provided by David Rudner at the Harvard Medical School, Boston, MA). pBM001 has a pDR183 backbone to integrate the plasmid into the *lacA* locus combined with a fragment from pDR111 that carries the Hyperspank promoter, the multiple-cloning site, and the Lac repressor. The FtsZ-GFP strain was created with the plasmid pX (69), which integrates genes into the *amyE* locus and expresses them from a xylose-inducible promoter. FtsZ was joined with GFPmut1 by

long-flanking homology (LFH) PCR and inserted into pX. For the construction of EzrA-GFP, we made use of the pSG1154 plasmid (70), which allows in-frame fusions to GFPmut1 and further expression under the control of a xylose-inducible promoter. For the independent overexpression of both flotillins and a third xylose-inducible gene, we decided to construct a bicistronic mRNA of *floA* and *floT* via LFH-PCR, which was integrated into the *lacA* locus with pBM001. The strain showed similar overexpression of *floA* and *floT* in the presence of IPTG compared to expression of a single gene, as determined by reverse transcription (RT)-PCR (data not shown).

Image analysis. Biofilms were documented using a Nikon SMZ 1500 stereoscope equipped with a Leica DFC295 color camera and Zeiss Axio Vision software. Final processing of the images was done with Photoshop. For microscopy, an overnight culture was diluted 1:20 in MSgg medium and grown at 30°C with agitation at 200 rpm until reaching the desired growth stage. If necessary, inducers were added to the culture as stated in the figure legends. Prior to analysis, 1 μM FM4-64 (Invitrogen, Carlsbad, CA) was added to stain the membrane, and Hoechst 33342 was added to a final concentration of 1 μg/ml to stain the DNA. For static images, cells were fixed with 4% paraformaldehyde for 7 min and washed with phosphate-buffered saline (PBS) several times. Finally, cells were spotted on a microscopic slide covered with a 1% agarose pad made with PBS. Images were captured with a Leica DMI6000B microscope equipped with a Leica CRT6000 illumination system coupled with a Leica DFC630FX color camera. Deconvolution was performed with a software algorithm of the LAS AF software. Fluorescence quantification and generation of color spectra were performed with Fiji. Images were processed with Leica LAS AF software and Photoshop.

Flow cytometry. For flow cytometry analysis, 3-day-old biofilms were detached from the agar surface, resuspended in PBS, and mildly sonicated (power output of 0.7 and cycle of 50%) in order to separate cells from extracellular matrix material. Subsequently, cells were fixed with 4% paraformaldehyde for 7 min and washed several times. For analysis, cells were diluted 1:1,000 in PBS. Analysis was carried out with the benchtop MACS-quant analyzer (Miltenyi Biotech, Germany). YFP signals were detected
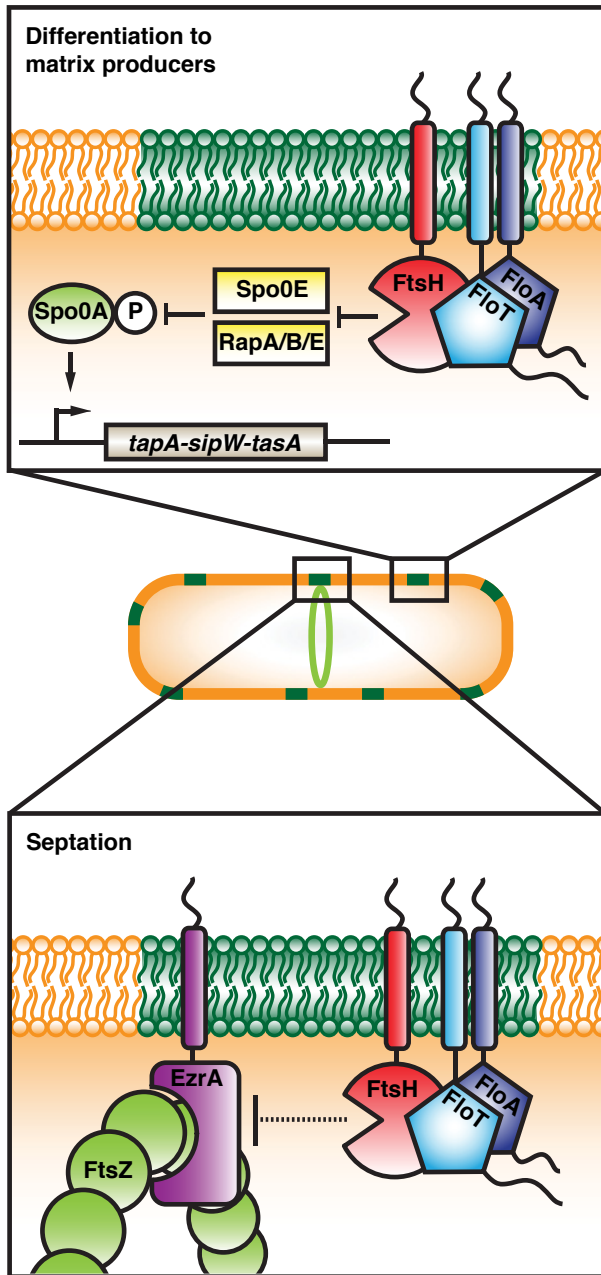
FIG 7 Hypothetical model for the dual role of FtsH activity in *B. subtilis* membrane microdomains. In the membrane microdomains (green), the flotillins FloA and FloT regulate the protease activity of FtsH. The upper panel represents a situation with FtsH degrading regulatory phosphatases, which ultimately leads to biofilm formation via activation of the TasA operon. During cell division (lower panel), FtsH might also degrade the negative regulator for Z-ring formation, EzrA, by a yet unknown mechanism (referred to as dashed lines) and thus contribute indirectly to formation of the division septum.

using a 488-nm laser with the corresponding 525/50-nm filter. The photomultiplier voltage was set at 462 V. For each sample, 50,000 nongated cells were measured. Data analysis was performed using the FlowJo v 9.5.1 software (Tree Star, Inc., Ashland, OR).

Western blot analysis. For extraction of whole-cell fractions, cells were grown in liquid MSgg medium at 30°C; the length of cultivation

varied according to the corresponding experiment. Cells were collected by centrifugation and subsequently lysed with 1 mg/ml lysozyme at 37°C for 30 min. After lysozyme treatment, samples were subjected to SDS-PAGE, and proteins were detected by Coomassie staining. The extracellular fraction was extracted as previously described (37, 71) with minor modifications. Briefly, cells were grown in liquid MSgg medium without agitation at 30°C. The floating biofilm, including the liquid medium, was recovered and mild sonication was applied to separate the extracellular fraction from the cells. After that, cells were pelleted and the supernatant was filter sterilized (0.2-μm pore size). The extracellular proteins in the supernatant were precipitated with trichloroacetic acid with a final concentration of 10% (vol/vol). Precipitated proteins were harvested by centrifugation and taken up in 1$\times$ SDS sample buffer. Immunoblot analysis was performed according to standard protocols. Antibodies were purchased from Invitrogen (anti-GFP) and Bio-Rad (anti-rabbit IgG, horseradish peroxidase [HRP] conjugate). The TasA antibody was kindly provided by Kürsad Turgay (Freie University of Berlin, Germany). The FtsH antibody was a kind gift from Thomas Wiegert (Hochschule Zittau/Görlitz, Germany).

SUPPLEMENTAL MATERIAL

ACKNOWLEDGMENTS

REFERENCES

1. **Matsumoto K, Kusaka J, Nishibori A, Hara H.** 2006. Lipid domains in bacterial membranes. Mol. Microbiol. **61:**1110–1117.
2. **Rudner DZ, Losick R.** 2010. Protein subcellular localization in bacteria. Cold Spring Harb. Perspect. Biol. **2:**a000307. doi:10.1101/cshperspect.a000307.
3. **Simons K, Gerl MJ.** 2010. Revitalizing membrane rafts: new tools and insights. Nat. Rev. Mol. Cell Biol. **11:**688–699.
4. **Simons K, Ikonen E.** 1997. Functional rafts in cell membranes. Nature **387:**569–572.
5. **Simons K, Sampaio JL.** 2011. Membrane organization and lipid rafts. Cold Spring Harb. Perspect. Biol **3:**a004697. doi:10.1101/cshperspect.a004697.
6. **López D, Kolter R.** 2010. Functional microdomains in bacterial membranes. Genes Dev. **24:**1893–1902.
7. **Dempwolff F, Moller HM, Graumann PL.** 2012. Synthetic motility and cell shape defects for deletions of flotillin/reggie paralogs in *Bacillus subtilis* and interplay with NfeD proteins. J. Bacteriol. **194:**4652–4661.
8. **Donovan C, Bramkamp M.** 2009. Characterization and subcellular localization of a bacterial flotillin homologue. Microbiology **155:**1786–1799.
9. **Zhao F, Zhang J, Liu YS, Li L, He YL.** 2011. Research advances on flotillins. Virol. J. **8:**479–484.
10. **Stuermer CA.** 2010. The reggie/flotillin connection to growth. Trends Cell Biol. **20:**6–13.
11. **Morrow IC, Parton RG.** 2005. Flotillins and the PHB domain protein family: rafts, worms and anaesthetics. Traffic **6:**725–740.

12. **Stuermer CA.** 2011. Reggie/flotillin and the targeted delivery of cargo. J. Neurochem. **116:**708–713.

13. **Allen JA, Halverson-Tamboli RA, Rasenick MM.** 2007. Lipid raft microdomains and neurotransmitter signalling. Nat. Rev. Neurosci. **8:**128–140.

14. **Kokubo H, Lemere CA, Yamaguchi H.** 2000. Localization of flotillins in human brain and their accumulation with the progression of Alzheimer's disease pathology. Neurosci. Lett. **290:**93–96.

15. **Girardot N, Allinquant B, Langui D, Laquerrière A, Dubois B, Hauw JJ, Duyckaerts C.** 2003. Accumulation of flotillin-1 in tangle-bearing neurones of Alzheimer's disease. Neuropathol. Appl. Neurobiol. **29:**451–461.

16. **Koch JC, Solis GP, Bodrikov V, Michel U, Haralampieva D, Shypitsyna A, Tönges L, Bähr M, Lingor P, Stuermer CA.** 2013. Upregulation of reggie-1/flotillin-2 promotes axon regeneration in the rat optic nerve in vivo and neurite growth in vitro. Neurobiol. Dis. **51:**168–176.

17. **Schulte T, Paschke KA, Laessing U, Lottspeich F, Stuermer CA.** 1997. Reggie-1 and reggie-2, two cell surface proteins expressed by retinal ganglion cells during axon regeneration. Development **124:**577–587.

18. **Munro S.** 2003. Lipid rafts: elusive or illusive? Cell **115:**377–388.

19. **Butcher BG, Helmann JD.** 2006. Identification of *Bacillus subtilis* sigma-dependent genes that provide intrinsic resistance to antimicrobial compounds produced by bacilli. Mol. Microbiol. **60:**765–782.

20. **Bach JN, Bramkamp M.** 2013. Flotillins functionally organize the bacterial membrane. Mol. Microbiol. **88:**1205–1217.

21. **Dempwolff F, Möller HM, Graumann PL.** 2012. Synthetic motility and cell shape defects associated with deletions of flotillin/reggie paralogs in *Bacillus subtilis* and interplay of these proteins with NfeD proteins. J. Bacteriol. **194:**4652–4661.

22. **Yepes A, Schneider J, Mielich B, Koch G, García-Betancur JC, Ramamurthi KS, Vlamakis H, López D.** 2012. The biofilm formation defect of a *Bacillus subtilis* flotillin-defective mutant involves the protease FtsH. Mol. Microbiol. **86:**457–471.

23. **Hamon MA, Lazazzera BA.** 2001. The sporulation transcription factor Spo0A is required for biofilm development in *Bacillus subtilis*. Mol. Microbiol. **42:**1199–1209.

24. **Lopez D, Vlamakis H, Kolter R.** 2009. Generation of multiple cell types in *Bacillus subtilis*. FEMS Microbiol. Rev. **33:**152–163.

25. **Le AT, Schumann W.** 2009. The Spo0E phosphatase of *Bacillus subtilis* is a substrate of the FtsH metalloprotease. Microbiology **155:**1122–1132.

26. **Haeusser DP, Garza AC, Buscher AZ, Levin PA.** 2007. The division inhibitor EzrA contains a seven-residue patch required for maintaining the dynamic nature of the medial FtsZ ring. J. Bacteriol. **189:**9001–9010.

27. **Haeusser DP, Schwartz RL, Smith AM, Oates ME, Levin PA.** 2004. EzrA prevents aberrant cell division by modulating assembly of the cytoskeletal protein FtsZ. Mol. Microbiol. **52:**801–814.

28. **Singh JK, Makde RD, Kumar V, Panda D.** 2007. A membrane protein, EzrA, regulates assembly dynamics of FtsZ by interacting with the C-terminal tail of FtsZ. Biochemistry **46:**11013–11022.

29. **Branda SS, González-Pastor JE, Ben-Yehuda S, Losick R, Kolter R.** 2001. Fruiting body formation by *Bacillus subtilis*. Proc. Natl. Acad. Sci. U. S. A. **98:**11621–11626.

30. **López D, Kolter R.** 2010. Extracellular signals that define distinct and coexisting cell fates in *Bacillus subtilis*. FEMS Microbiol. Rev. **34:**134–149.

31. **Vlamakis H, Chai Y, Beauregard P, Losick R, Kolter R.** 2013. Sticking together: building a biofilm the *Bacillus subtilis* way. Nat. Rev. Microbiol. **11:**157–168.

32. **Branda SS, González-Pastor JE, Dervyn E, Ehrlich SD, Losick R, Kolter R.** 2004. Genes involved in formation of structured multicellular communities by *Bacillus subtilis*. J. Bacteriol. **186:**3970–3979.

33. **Kearns DB, Chu F, Branda SS, Kolter R, Losick R.** 2005. A master regulator for biofilm formation by *Bacillus subtilis*. Mol. Microbiol. **55:**739–749.

34. **Chai L, Romero D, Kayatekin C, Akabayov B, Vlamakis H, Losick R, Kolter R.** 2013. Isolation, characterization, and aggregation of a structured bacterial matrix precursor. J. Biol. Chem. **288:**17559–17568.

35. **Stöver AG, Driks A.** 1999. Control of synthesis and secretion of the *Bacillus subtilis* protein YqxM. J. Bacteriol. **181:**7065–7069.

36. **Stöver AG, Driks A.** 1999. Regulation of synthesis of the *Bacillus subtilis* transition-phase, spore-associated antibacterial protein TasA. J. Bacteriol. **181:**5476–5481.

37. **Branda SS, Chu F, Kearns DB, Losick R, Kolter R.** 2006. A major protein component of the *Bacillus subtilis* biofilm matrix. Mol. Microbiol. **59:**1229–1238.

38. **Romero D, Aguilar C, Losick R, Kolter R.** 2010. Amyloid fibers provide structural integrity to *Bacillus subtilis* biofilms. Proc. Natl. Acad. Sci. U. S. A. **107:**2230–2234.

39. **Romero D, Vlamakis H, Losick R, Kolter R.** 2011. An accessory protein required for anchoring and assembly of amyloid fibres in *B. subtilis* biofilms. Mol. Microbiol. **80:**1155–1168.

40. **McLoon AL, Guttenplan SB, Kearns DB, Kolter R, Losick R.** 2011. Tracing the domestication of a biofilm-forming bacterium. J. Bacteriol. **193:**2027–2034.

41. **Chu F, Kearns DB, Branda SS, Kolter R, Losick R.** 2006. Targets of the master regulator of biofilm formation in *Bacillus subtilis*. Mol. Microbiol. **59:**1216–1228.

42. **López D, Fischbach MA, Chu F, Losick R, Kolter R.** 2009. Structurally diverse natural products that cause potassium leakage trigger multicellularity in *Bacillus subtilis*. Proc. Natl. Acad. Sci. U. S. A. **106:**280–285.

43. **Quadri LE, Weinreb PH, Lei M, Nakano MM, Zuber P, Walsh CT.** 1998. Characterization of Sfp, a *Bacillus subtilis* phosphopantetheinyl transferase for peptidyl carrier protein domains in peptide synthetases. Biochemistry **37:**1585–1595.

44. **Reuter K, Mofid MR, Marahiel MA, Ficner R.** 1999. Crystal structure of the surfactin synthetase-activating enzyme sfp: a prototype of the 4′-phosphopantetheinyl transferase superfamily. EMBO J. **18:**6823–6831.

45. **Schumann W.** 1999. FtsH—a single-chain charonin? FEMS Microbiol. Rev. **23:**1–11.

46. **Ito K, Akiyama Y.** 2005. Cellular functions, mechanism of action, and regulation of FtsH protease. Annu. Rev. Microbiol. **59:**211–231.

47. **Bieniossek C, Schalch T, Bumann M, Meister M, Meier R, Baumann U.** 2006. The molecular architecture of the metalloprotease FtsH. Proc. Natl. Acad. Sci. U. S. A. **103:**3066–3071.

48. **Bieniossek C, Niederhauser B, Baumann UM.** 2009. The crystal structure of apo-FtsH reveals domain movements necessary for substrate unfolding and translocation. Proc. Natl. Acad. Sci. U. S. A. **106:** 21579–21584.

49. **Janska H, Kwasniak M, Szczepanowska J.** 2013. Protein quality control in organelles—AAA/FtsH story. Biochim. Biophys. Acta **1833:**381–387.

50. **Tatsuta T, Langer T.** 2009. AAA proteases in mitochondria: diverse functions of membrane-bound proteolytic machines. Res. Microbiol. **160:** 711–717.

51. **Wehrl W, Niederweis M, Schumann W.** 2000. The FtsH protein accumulates at the septum of *Bacillus subtilis* during cell division and sporulation. J. Bacteriol. **182:**3870–3873.

52. **Barák I, Prepiak P, Schmeisser F.** 1998. MinCD proteins control the septation process during sporulation of *Bacillus subtilis*. J. Bacteriol. **180:** 5327–5333.

53. **Feucht A, Errington J.** 2005. ftsZ mutations affecting cell division frequency, placement and morphology in *Bacillus subtilis*. Microbiology **151:** 2053–2064.

54. **Reeve JN, Mendelson NH, Coyne SI, Hallock LL, Cole RM.** 1973. Minicells of Bacillus subtilis. J. Bacteriol. **114:**860–873.

55. **Bi EF, Lutkenhaus J.** 1991. FtsZ ring structure associated with division in *Escherichia coli*. Nature **354:**161–164.

56. **Errington J, Daniel RA, Scheffers DJ.** 2003. Cytokinesis in bacteria. Microbiol. Mol. Biol. Rev. **67:**52–65.

57. **Bi E, Lutkenhaus J.** 1993. Cell division inhibitors SulA and MinCD prevent formation of the FtsZ ring. J. Bacteriol. **175:**1118–1125.

58. **Weart RB, Lee AH, Chien AC, Haeusser DP, Hill NS, Levin PA.** 2007. A metabolic sensor governing cell size in bacteria. Cell **130:**335–347.

59. **Brown DA.** 2002. Isolation and use of rafts. Curr. Protoc. Immunol. Chapter 11:Unit 11.10. doi:10.1016/j.cell.2007.05.043.

60. **Lingwood D, Simons K.** 2007. Detergent resistance as a tool in membrane research. Nat. Protoc. **2:**2159–2165.

61. **Levin PA, Kurtser IG, Grossman AD.** 1999. Identification and characterization of a negative regulator of FtsZ ring formation in *Bacillus subtilis*. Proc. Natl. Acad. Sci. U. S. A. **96:**9642–9647.

62. **Kang MS, Kim SR, Kwack P, Lim BK, Ahn SW, Rho YM, Seong IS, Park SC, Eom SH, Cheong GW, Chung CH.** 2003. Molecular architecture of the ATP-dependent CodWX protease having an N-terminal serine active site. EMBO J. **22:**2893–2902.

63. **Zellmeier S, Zuber U, Schumann W, Wiegert T.** 2003. The absence of FtsH metalloprotease activity causes overexpression of the sigmaW-controlled pbpE gene, resulting in filamentous growth of *Bacillus subtilis*. J. Bacteriol. **185:**973–982.

64. **Hardwood CR, Cutting SM.** 1990. Molecular biological methods for *Bacillus*. Wiley, New York, NY.
65. **Dubnau D.** 1991. Genetic competence in *Bacillus subtilis*. Microbiol. Rev. **55:**395–424.
66. **Yasbin RE, Young FE.** 1974. Transduction in *Bacillus subtilis* by bacteriophage SPP1. J. Virol. **14:**1343–1348.
67. **Britton RA, Eichenberger P, Gonzalez-Pastor JE, Fawcett P, Monson R, Losick R, Grossman AD.** 2002. Genome-wide analysis of the stationary-phase sigma factor (sigma-H) regulon of *Bacillus subtilis*. J. Bacteriol. **184:** 4881–4890.
68. **Nakano S, Küster-Schöck E, Grossman AD, Zuber P.** 2003. Spx-dependent global transcriptional control is induced by thiol-specific oxidative stress in *Bacillus subtilis*. Proc. Natl. Acad. Sci. U. S. A. **100:** 13603–13608.
69. **Kim L, Mogk A, Schumann W.** 1996. A xylose-inducible *Bacillus subtilis* integration vector and its application. Gene **181:**71–76.
70. **Lewis PJ, Marston AL.** 1999. GFP vectors for controlled expression and dual labelling of protein fusions in *Bacillus subtilis*. Gene **227:**101–110.
71. **Kobayashi K, Iwano M.** 2012. BslA(YuaB) forms a hydrophobic layer on the surface of *Bacillus subtilis* biofilms. Mol. Microbiol. **85:**51–66.